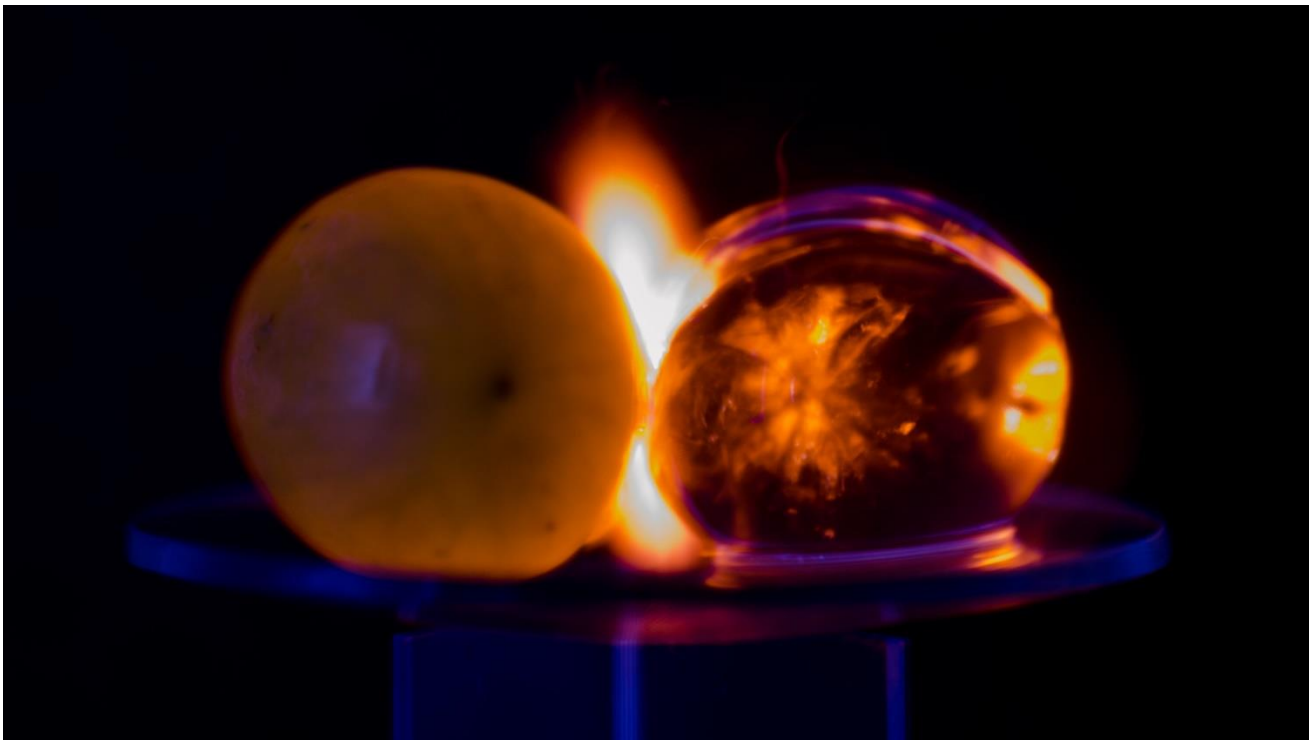

The Plasma Experiment

EXPERIMENTAL LAB ONE
TRINITY COLLEGE DUBLIN

Alexandra Mulholland | 3rd Year Astrophysics | 15/11/2019

Table of Contents

1. Abstract

Within this investigation, gas-filled tubes were utilised to investigate the behaviour of current through the plasma produced. The purpose of this investigation was two-fold. Firstly, the electron charge to mass ratio was estimated by measuring the values of current for increasing values of voltage across an 884 tube of argon gas. By plotting this collector voltage against current to the three-halves power, $\frac{e}{m}$ was found from the gradient of the linear section of the graph, which occurred at lower voltages. The expected ratio is around $1.76 \times 10^{11} C/kg$, but from the gradient of our plot, the value was found to be $5.96 \times 10^{11} C/kg$ (possible sources of error are considered later in section 5). Furthermore, within this first section of the experiment, the Child-Langmuir portion of this graph was used to determine the ionisation potential of argon. The expected value is $15.7V$ [10]. From the data, this value was approximately $17.57 \pm 0.59V$ beyond which the current between the electrodes is no longer space-charge limited (described by the Child-Langmuir law), but temperature-limited and hence governed by the Richardson-Dushman relation. In part 2 of this investigation, a Langmuir Probe was utilised to take measurements of voltage and current, from which the electron temperature and electron density of the plasma could be deduced. The tube used for this section was a gas triode (Z300T) of argon gas. By plotting the probe current versus the probe voltage in the range of -9V to +15V and determining the saturation current, the electron density was found to be $1.936 \times 10^{16} \pm 6.26 \times 10^{14} m^{-3}$- similar to the result from Robert L. Merlino [9] which was $1 \times 10^{16} m^{-3}$. The natural logarithm of the probe current was then calculated and plotted as a function of probe voltage- from the gradient, the electron temperature could be identified as about $8343.79 \pm 206.11K$ which is $\cong 0.72 \pm 0.02eV$ (about half of that deduced by Merlino). The use of an argon gas-filled tube for both parts was beneficial in both its effectiveness of creating and demonstrating the behaviour of plasma parameters and the fact it is comparably easy to ionise. It is appropriate in a laboratory setting due to its low cost (it is very common), high efficiency, and low breakdown voltage. The results obtained from this experiment could be amended through repetition: approaching the experiment with a greater understanding of the issues associated with polar reversal of the probe and voltmeter, as well as those associated with the ammeter prefixes would yield closer results to those expected.

2. Scientific Background

2.1- Part 1

To produce the plasma whose properties are investigated throughout this experiment, argon gas-filled tubes were used. By applying a potential difference across the gas, i.e. subjecting the inert element to an electric field, the gas will become ionised and so is now in a quasi-neutral mix of electrons and ions.

Part one of this investigation involved the determination of the ionisation potential of Argon by applying a potential difference across a tube filled with the element. The ionisation potential is defined by the energy required to remove an electron from the argon atom. The voltage, which was supplied by a cylindrical anode, was varied from low to high values and the corresponding currents were measured. This involved investigating the relationship which describes the limit on the maximum current density in a vacuum between two relatively large (almost infinitely sized for the purposes of calculation) parallel electrodes compared to the region of space between them, and the potential difference at which this maximum current occurs. This relationship is known as the Child-Langmuir Law (equation 1 below) and governs space-charge limited flow. [1] Space-charge is usually a term used to refer to the excess of electric charge being treated as a continuum over a region, like a cloud, as opposed to point-like charges. This region is that between the two electrode plates, one being a cathode and one an anode. The tube used in this investigation was an 884 tube: an argon-filled thermionic triode. This means there are 3 electrodes within the tube. In this first section of the experiment, the grid, labelled 5 in figure 1, is attached to plate 3 to convert the triode to a diode.

[2] The charge of these two plates can be attributed to this source being an electrolytic cell, one which converts electrical energy to chemical. The cathode in this case is therefore the source of the electrons. Heating of the cathode plate results in Thermionic Emission and electrons are released once the work function of the cathode material is reached. Subsequently, the electrons "evaporate" into the region between the electrodes. When a positive potential difference is applied between the two plates, the cathode is biased to $0V$, while the anode is biased towards positive voltages [4]. The electrons will be accelerated in a low-density beam towards the positive anode, creating a current between the plates. This current moving to the right constitutes a conventional positive current density in the opposite direction [3]. The circuit diagram illustrating the setup used is shown in figure 1 below, and each component explained in section 3.1. [10]

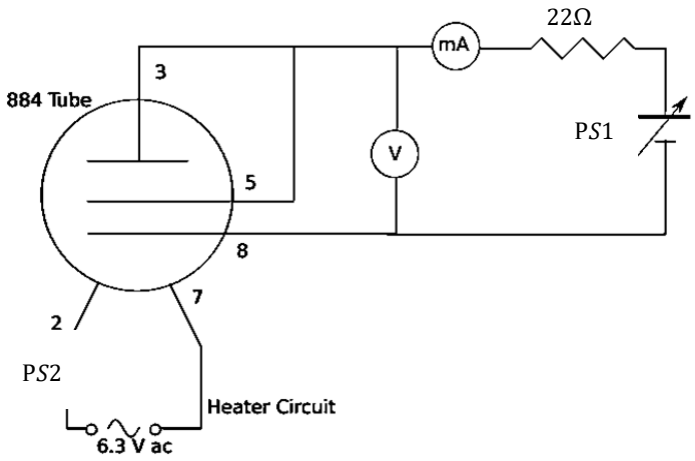

Figure 1: Diagram of the circuit used in part 1.

Initially, at low voltages, the result is that the evacuated glass tube, which contains the electrodes, acts as a diode (i.e. it allows current to flow in one direction and hinders flow of current in the other). This is because in this low-voltage regime, the electrons emitted will inhabit the region between the cathode and anode and thus hinder the overall potential difference. The region is therefore space-charge limited, and so the Child-Langmuir law describes the relationship between the voltage and current. Increasing the potential difference means the current is now limited by the 'evaporation' of electrons from the cathode, as all the electrons will be carried to the anode.

This region is thus known as the temperature-limited region and is governed by a different law known as the Richardson-Dushman relationship, which relates the current density produced by a material to its work function and temperature.

Once a certain value of the potential difference is attained, the tube current and voltage no longer fulfil the relationship described by the Child-Langmuir law. Instead, the current will plateau with increasing voltage beyond this point, as the electrons emitted from the cathode obtain enough energy to ionise the argon gas. The voltage at which this occurs is known as the breakdown voltage and can be ascertained from a plot of the collector voltage versus the tube current to the power of 2/3. The difference between the breakdown voltage and the voltage at which the corresponding current is of zero value is known as the ionisation potential. This will be clarified below. A graph of the expected results is shown in figure 2. [5]

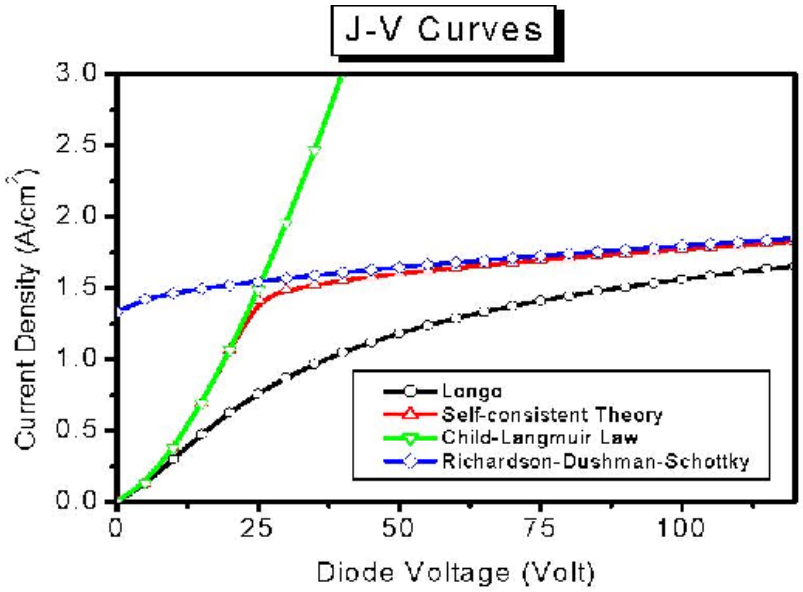

Figure 2: Plot of the current density versus voltage trends for the Child-Langmuir, Richardson-Dushman and experimental result expectation shown in green, blue and red respectively.

Within the region of fulfilment of the Child-Langmuir law, there are two assumptions which are made for the relationship to be valid. The first is, as mentioned previously, the space between the two electrodes is significantly smaller than the sizes of said electrodes- to a point where the diode is assumed to have an infinite extension in the x-y direction. Thus, the fringing effects on the edges of the plates can be neglected. Secondly, the particles move linearly across the gap at speeds which are non-relativistic.

The Child-Langmuir Law is described by equation (2.1) below, where the derivation for this equation has been explicitly completed in the preceding lines [6].

From the differential form of Gauss' Law of electric fields, one can derive Poisson's equation for the electric potential (which acts in the z direction) between the electrodes:

$$\frac{d^2V}{dz^2} = \frac{-\rho}{\varepsilon_0}$$

Where V is the electric potential, ρ is the charge density (Cm^{-3}) and ε_0 is the permittivity of free space. Due to the assumption of infinite extension of the plates in the x-y direction, the current density is in the z direction and can be written as follows:

$$J(z) = \rho(z)v(z) = -J_{CL}$$

As mentioned, the current moving from the cathode to the anode constitutes a conventional current moving in the opposite direction, hence the negative sign on the space charge-limited current density, J_{CL}. Here, $v(z)$ is the average velocity of the electrons in the z-direction. Due to the principle of the conservation of charge, this charge density is constant in said direction between the two electrodes, thus, the principle of the conservation of energy can be applied:

$$\frac{1}{2}mv^2 = eV \quad \text{thus} \quad v = \sqrt{\frac{2eV}{m}}$$

Whereby m is the mass of an electron, e is the charge of the electron and V is the potential difference through which the electron is being accelerated (i.e. the potential difference between the two electrodes). Here we have assumed the electrons are initially at rest in the cathode. Hence, the kinetic energy of the electrons is equal to the work done on the electrons by the electric field applied. Substituting the velocity into the expression for current density, one obtains:

$$\rho(z) = -\frac{J_{CL}}{\sqrt{2eV/m}}$$

Substituting this expression into Poisson's equation, a second-order non-linear differential equation is acquired:

$$\frac{d^2V}{dz^2} = \frac{J_{CL}}{\varepsilon_0\sqrt{2eV/m}}$$

In order to solve this equation, boundary conditions must be applied. These have been briefly mentioned, however, their importance is highlighted here. The two boundary conditions applied state that the potential difference at the cathode (i.e. at z=0) is zero, and the change in this applied potential difference with z is also zero at this point. The solution to this second order differential is therefore:

$$V(z) = V_0\left(\frac{z}{D}\right)^{4/3}$$

Here, V_0 is the bias potential- the potential needed to be applied for the diode to function. This equation states that the potential difference across the electrode plates will decrease with the power of $\frac{4}{3}$ of the fractional distance across the space between them.

Now we can find an expression for the volume charge density by differentiating the above expression twice with respect to z one will find:

$$\frac{d^2V}{dz^2} = \frac{4}{9D^2}V_0\left(\frac{z}{D}\right)^{-2/3}$$

And so, the charge density from Poisson's equation is:

$$\rho(z) = -\frac{4}{9D^2}V_0\varepsilon_0\left(\frac{D}{z}\right)^{2/3}$$

Therefore, the space charge-limited current density is this expression multiplied by the electron velocity, factoring in the convention for direction:

$$J_{CL} = \frac{4V_0\varepsilon_0}{9D^2}\left(\frac{D}{z}\right)^{2/3}\sqrt{\frac{2eV}{m}}$$

Putting this expression in terms of the bias potential by substituting the expression for V, one obtains the final expression for the Child-Langmuir law in terms of current density.

$$J_{CL} = \frac{4\varepsilon_0}{9D^2}\sqrt{\frac{2e}{m}}{V_0}^{3/2}$$

This expression was modified to be in terms of current, I, within the space of the electrode:

$$I = \left[2\pi\varepsilon_0\frac{4L}{9R}\sqrt{2e/m}\right]{V_0}^{3}/_{2} \qquad (2.1)$$

For the purposes of this investigation, the equation was rearranged, and the resultant plot was V versus $I^{\frac{2}{3}}$. The rearranged equation is equation (2.2).

$$V = \left[2\pi\varepsilon_0\frac{4L}{9R}\sqrt{2e/m}\right]^{-\frac{2}{3}}I^{2}/_{3} \qquad (2.2)$$

2.2- Part 2

For the second part of this experiment, a common diagnostic in plasma physics known as the Langmuir probe was utilised in order to determine the plasma electron density and electron temperature, T_e. This plasma parameter is defined as the temperature of the distribution of the group of electrons' velocities within the plasma. We can define this parameter in such a way as we know the velocities of the group of electrons follow a Maxwellian distribution. The tube used in this case was a $Z300T$ tube- one which is also a gas triode filled with argon. Rather than conversion of the triode to a diode as was performed in part 1 of this investigation, the triode consisted of a trigger anode, a cathode and a second anode which acted as the Langmuir probe in between the other two electrodes. [12] The probe is immersed within the plasma biased to the voltage across the probe with respect to the reference anode. The discharge occurs by applying a DC voltage between said electrodes, with the anode being cylindrical and the cathode being a ring shape. The voltage is varied from negative to positive values and the corresponding current through the probe is measured. This current is a combination of the electron and ion currents, which will be explained shortly.

By doing so, one should observe a trend such as the one shown in figure 4. [7] In this case, both the electrons and positive ions can contribute to the current to the probe. This is dependent on the polarity and size of the voltage, and so this was varied accordingly. Figure 3 shows the circuit diagram for this part of the investigation. [10]

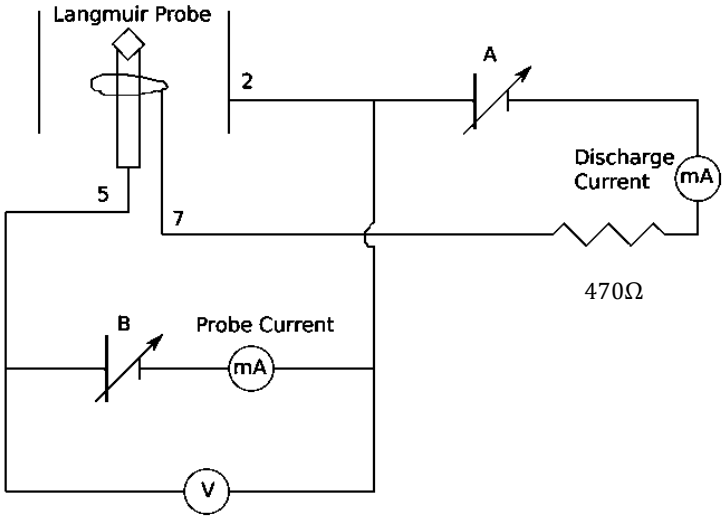

Figure 3: Circuit diagram of the set up for part 2 of the investigation

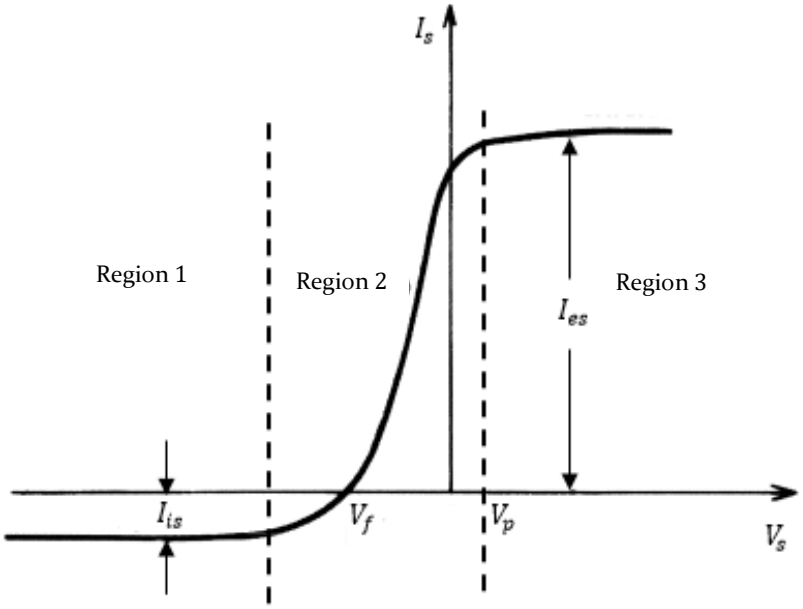

Figure 4: Diagram showing the I-V characteristic one would expect to see when increasing the voltage to the Langmuir probe in a Z300T argon-filled gas triode.

Something to note before analysing the trend shown in figure 4 is a fundamental property of plasma upon inserting a test charge into the plasma. If one were to insert a positive test charge, negatively charged particles will form a negative-space-charge cloud around the test charge. This negative sheath, as it is known, is such that it will eradicate the electric field influence of the test charge on the plasma surrounding the negative sheath. The distance over which the test charge's electric field is screened out is known as the Debye length (equation 2.3): a scale which is dependent on the plasma temperature and density. The same effect applies for a negative test charge, where instead a positive sheath is formed. A Langmuir probe essentially acts as a test charge and the potential of the probe will be shielded over the Debye length.

Due to these charged sheaths, it is no longer possible to attract surrounding oppositely charged particles, and so the current saturates. One will observe in the figure that there are two such regions of saturation, where the current is of constant value with increasing voltage.

$$\lambda_D = \sqrt{\frac{\varepsilon_0 k T_e}{n_e e^2}} \tag{2.3}$$

Whereby n_e is the electron density, k is Boltzmann's constant, T_e is the electron temperature and all other symbols have their usual meanings.

Furthermore, it should be noted that the electrons' and ions' velocities within the plasma follow a Maxwellian distribution, and so are considered to have a temperature.

Region 1 on the diagram represents the ion saturation region. Here, a relatively large negative potential (with respect to the plasma) is applied to the probe. Positive ions are therefore attracted to the probe and form a positive-space-charge region, known as a positive sheath, while electrons are repelled. Only the most energetic electrons will overcome the repelling electric field of the probe. The electron current in the probe will therefore be zero, and the only current collected by the probe is that due to positive ions. This is the ion saturation current and is the lowest value of the current on the I-V plot, and is described by equation 2.4, where n_i and v_i are the ion densities and speeds respectively.

$$I_{is} = \frac{1}{4} e n_i v_i A \tag{2.4}$$

Beyond this point, the electron energies increase with bias potential. Hence, there is an exponential increase in the number which are sufficiently energetic to contribute to the electron current. This electron current contribution will eventually equal the ion saturation current (however opposite in polarity). The value of the bias voltage at which the curve crosses the x-axis, i.e. where the current is zero, is known as the floating potential V_f. Here, the probe draws equal ion and electron currents and so no net current is registered. The probe is referred to as 'electrically floating' [9]. [11] To clarify, it should be noted that within a plasma, the electrons have much higher thermal speeds when compared to the positive ions (due to the electrons' smaller masses). Therefore, despite the plasma being quasi-neutral (whereby the electron and ion densities are equal), the flux of each species upon introduction of an electrically isolated substrate to the plasma is unequal. That is, an electrically floating probe will draw a higher electron current due to the electrons reaching the probe sooner. The probe then begins to negatively charge with respect to the plasma: the sheath forms. The flux of electrons to the probe is thus diminished and eventually matches that of the ions. The floating potential is that at which this balance is achieved. One can think of this as the potential of the probe 'floating' to a value to obtain this equal flux.

Region 2 represents the region between the floating potential V_f and the plasma potential, V_p, known as the electron-retardation region, where electrons are partially repelled by the probe [8]. Here, slow, low-energy electrons are still repelled by the negative probe, however, the more energetic electrons reach the probe. One will observe that the higher the probe bias, i.e. the higher the applied voltage, the higher the probability of "catching" passing charges. Hence, the measured current increases with probe voltage, where electron current is now dominant.

In voltages below the plasma potential, the I-V characteristic is:

$$I \propto e^{\frac{eV}{kT_e}} \tag{2.5}$$

Where V is the bias voltage applied to the probe and the particles are assumed to obey Maxwellian behaviour.

The plasma potential, V_p, is the potential of the plasma with respect to the walls of the tube, i.e. the equipotential of the bulk of the plasma, which is not subject to the disturbances upon introduction of the probe. It is expected that this value will be of higher (more positive) voltage with respect to the walls of the probe, as one will observe in figure 4. This is explained by the fact that higher energy electrons will reach the walls first and, as stated, the bulk plasma is left with a slightly more positive space-charge.

[11] Region 3 of the figure illustrates the electron saturation region, where any further increase in the bias potential beyond V_p is merely contributing to the energy of the electrons, as oppose to the current, and the highest value of the current is known as the electron saturation current. This is the region whereby the Langmuir probe has a very large positive voltage with respect to the bulk of the plasma. The electron saturation current is given by equation 2.6 below, where A is the surface area of the probe, n_e is the electron density, v_e is the electron thermal speed and e is the charge of the electron.

$$I_{es} = en_eA\sqrt{\frac{kT_e}{2\pi m}} \tag{2.6}$$

3. Method

3.1- Part 1

The circuit used to execute this part of the experiment is shown in figure 1, where each instrument used is labelled. The 884 tube of Argon gas was connected to the power supply $PS1$, which produces a direct current voltage which can be varied. The cylindrical anode is $2.24cm$ in length with a radius of $0.15cm$. This was set at an output of $0.3V$ and $0.2A$, with the "Grob coarse" knob turned to the maximum setting to ensure the correct readings were taken and none were omitted. This was done as it was learned that the setting of the power supply meant the current was unable to increase further, hence the ammeter would only read a certain maximum value, which was much lower than the range of readings we were expecting to reach.

A second power supply, $PS2$, was connected to the heater circuit via the $6.3V$ alternating current output. This supply was set to a value of a $2A$ output and had a metre range of $35 - 350V$.
The tube was left to heat for five minutes, as one would observe an output current of $0.0A$ if not. To ensure the measurements were of acceptable accuracy, a test run was carried out, with a subsequent test plot of $I^{2/3}$ versus V. Once the expected trend for the results was verified, a larger range and smaller incremented data points were taken. It was decided to measure the current in mA for voltages ranging from $0V$ to $18V$. The corresponding current measurements were recorded and the values of $I^{2/3}$ were calculated. These were also recorded in mA. When calculating these values, care had to be taken as merely inputting the current in mA form into one's calculator results in a value which is a factor of 10 too small, therefore one should input the current in amps.
A graph of the collector voltage in V versus $I^{2/3}$ in mA was plotted within the ranges stated. Corresponding to the linear portion of this graph, a line of best fit was drawn both roughly and on origin. By determining the gradient of this line and solving equation (2.2), a value of $\frac{e}{m}$ could be found.

The value of the collector voltage at which this liner relation breaks down was then found, along with the value of this voltage at which the current is zero. The difference in these two values is the ionisation potential of Argon. This value was calculated and recorded.

3.2- Part 2

The second part of this investigation utilised the circuit shown in diagram 2. Here, both the direct current outputs of the second power supply were used labelled A and B. A is the output which produces the discharge voltage of range 35-350V, B indicates the probe voltage and ranges from 0 to 35V.
The discharge voltage from A was slowly increased until a purple glow is observed in the gas triode tube. This was observed to occur at around +140V. The discharge voltage was increased to a value of +175V, where a discharge current of 10.04mA was produced.
The probe in this instance is $5mm$ long (length is denoted by 'l' below) with a $0.35mm$ radius, r, thus the surface area of the probe, which was used in the calculations as 'A', is $\pi r^2 + 2\pi rl$. That is, the area of the base of the cylindrical probe plus the surface area of the length of the probe. This is therefore $\approx 1.138 \times 10^{-5} m^2$.

The probe current was measured in μA initially and recorded for probe voltages ranging from $-9V$ to $+15V$, in increments of $0.5V$. These increment sizes were decreased around areas where the probe current increased significantly for relatively small changes in probe voltage, known as the region of zero bias. The probe current versus the applied probe voltage data was then plotted.
In order to reverse the polarity of both the probe and the meters, the wires at the B output of $PS2$ were reversed. This was done at $0.0V$, where here the ammeter was set from μA to mA. This was because the ammeter could no longer read the currents in the μA setting as the currents at larger voltages was too high (and hence would result in error). From the plot, and subsequent plot of the natural logarithm of current versus the probe voltage, the saturation current, electron density and electron temperature of the plasma were determined.

4. Results

4.1- Part 1

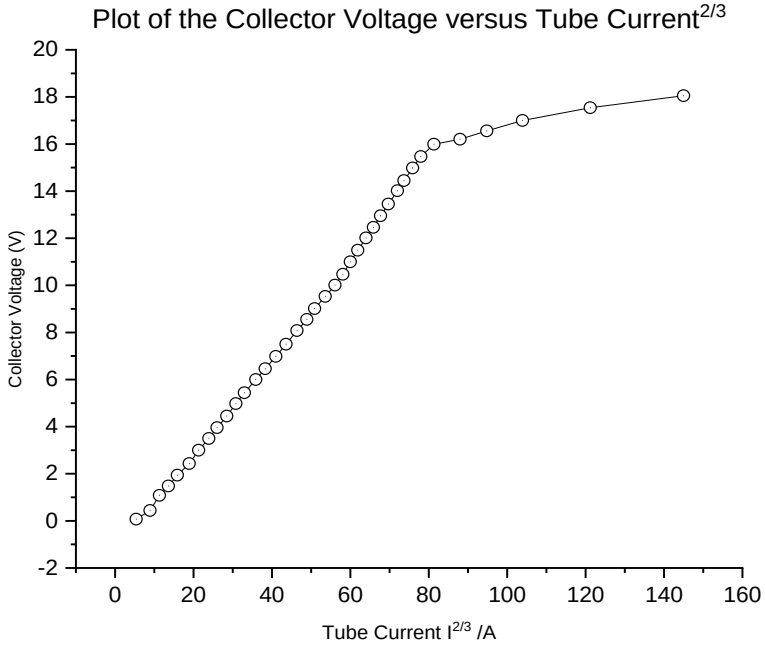

Figure 4.1.1: Plot of the voltage ranging from 0V to 18V across the 884 tube of argon against the current to the power of 2/3.

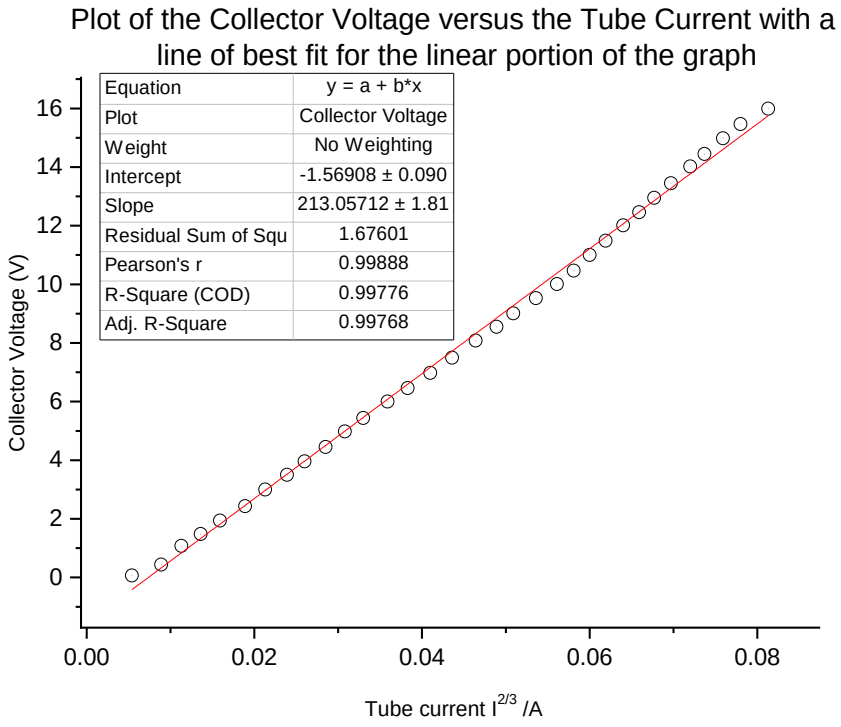

Figure 4.1.2: Plot of a line of best fit through the range of data shown in figure 4.1.1 which follows the Child-Langmuir law.

4.2- Part 2

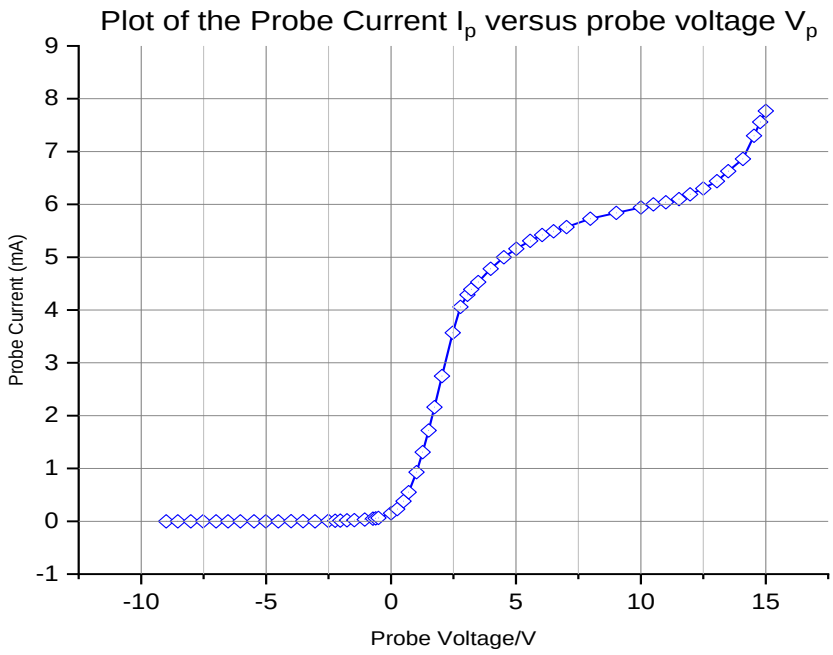

Figure 4.2.1: Plot of the measured current in milliamperes of the Langmuir probe versus the bias or probe voltage in volts.

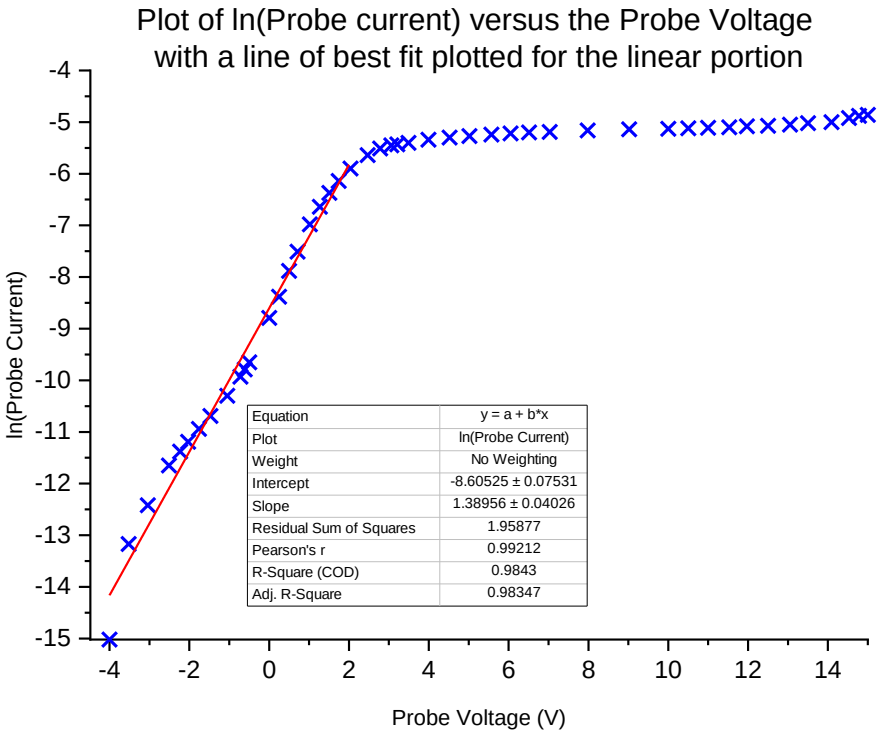

Figure 4.2.2: Plot of the natural logarithm of the current across the Langmuir probe versus the bias voltage. A line of best fit is plotted through the points which obey the relation stated in equation 2.5.

Error propagation

Error in the ionisation potential:

Breakdown Voltage V_{Br}: $16.0 \pm 0.05V$

Voltage at $I = 0$: $-1.57 \pm 0.09V$

Error in ionisation potential: $\sqrt{(\Delta V_{Br})^2 + (\Delta V(I = 0))^2} = \pm 0.10295 \ldots \approx \pm 0.1$

Error in the electron temperature:

The error is different for every point along the plot in figure 4.2.2. Using a random value on figure 4.2.2: $V = +2.04 \pm 0.05V$; ln(I)= -5.9; $I = 2.75A$.
$\Delta \ln(I) = \frac{\Delta I}{I} = \frac{\pm 0.05A}{2.75} = 0.01818 \ldots$

$$\Delta T_e = \sqrt{\left(\frac{\Delta V}{V}\right)^2 + \left(\frac{\Delta \ln(I)}{\ln(I)}\right)^2} \cdot |T_e| = \sqrt{\left(\frac{0.05}{2.04}\right)^2 + \left(\frac{0.01818 \ldots}{-5.9}\right)^2} \cdot |8343.79|$$

$$\Delta T_e = \pm 206.11K$$

5. Discussion

Figure 4.1.1 shows a plot of the variation of the tube current to the power of 2/3 versus the applied voltage. The voltage was varied from $0.07V$ to $18.05V$ (starting at $0V$ and increasing in $0.5V$ intervals proved difficult due to the sensitivity of the power supply, hence the voltage was increased in intervals $\approx 0.5 \pm 0.2V$). The plot follows the expected trend, where up to the breakdown voltage, $I^{2/3}$ increases linearly with applied voltage and is space-charge limited. Beyond this breakdown voltage, the region between the two electrodes no longer obeys the Child-Langmuir Law, but rather the Richardson-Dushman law, the trend for which is shown in figure 2. The line plateaus around an applied voltage of $16.0 \pm 0.05V$ (the breakdown voltage), and here the region is limited by temperature. The breakdown voltage minus the voltage at which the current is zero is the ionisation potential of Argon. Here, the voltage at which the current was zero (from the intercept value shown in figure 4.1.2) was around $-1.57 \pm 0.09V$, hence the ionisation potential of Argon was found to be $\approx 17.57 \pm 0.1V$. This is within an acceptable range of the expected value of $15.7V$ [4].

Using the line of best fit calculations (figure 4.1.2) generated by 'LoggerPro', along with equation 2.2, the electron charge to mass ratio could then be determined. This line of best fit represents the trend within which the Child-Langmuir Law is obeyed. The analytic magnitude of the value is $\frac{1.6\times10^{-19}}{9.11\times10^{-31}} = 1.76 \times 10^{11} C/kg$. The gradient of the graph is $\left(2\pi\varepsilon_0 \frac{4L}{9R}\sqrt{\frac{2e}{m_e}}\right)^{-2/3} = 1.38956 \pm 0.04\ A^{2/3}V^{-1}$. Therefore, rearranging this, one obtains the experimental value of e/m to be $\approx 5.96 \times 10^{11} C/kg$. Although larger than expected, this is quite close to the accepted value.

Figure 4.2.1 shows the I-V characteristic curve for the Langmuir probe within the $Z300T$ tube. The voltage applied to the probe was increased from $-9V$ to $+15V$. One can see the trend is of similar shape to figure 4 with the exception that the results from the experiment go beyond the electron saturation region. This is the exponentially increasing current through the probe with voltage across the probe beyond about $11 \pm 0.5V$. It is unclear why this trend occurs but is perhaps a result of the applied voltage being too large for the equipment used in this investigation.

When looking as we had done in section 2.2, we can see that the ion saturation region has an extremely small magnitude for the ion saturation current, as the electron current is zero. Upon review of this investigation, it would be beneficial to enhance the image to determine at which value of current this region occurs. The scale of measurement set on the ammeter was in microamps, with the lowest value collected in the data before the floating potential being $-2.4 \pm 0.1\mu A$ and the highest $-0.7 \pm 0.1\mu A$. The ion saturation current is then predicted to be somewhere within this range. Results from Robert L. Merlino [9] predict this value to be at $30\mu A$, a comparably large difference but small generally. This value represents the positive ion current. The diminutive size of this current can be explained by the fact that the ion current is small as outlined in equation 2.4, where the speed of the ions is significantly smaller relative to that of the electrons.

Further increase in the potential difference then leads to the floating potential at a value of approximately $0 \pm 0.5V$. Here, the electron current is now equal to the ion saturation current. This is therefore the potential at which the current is equal to zero, as no net current is registered by the probe because the probe has 'floated' to a negative potential to deter negative electrons and attract more positive ions. Thus, the flux of each reaching the probe is equal. The value obtained in this investigation contrasts with ref[9], which was $\cong -5V$. This is a highly differing result which could be due to a mistiming in the reversal of the polarity of the probe and the equipment.

Beyond the floating potential, the electron retardation region is as expected, with an increase in the current through the probe with voltage across it described by equation 2.5. Here, the polarity of the probe has been reversed and is now positive, thus attracting electrons to the probe. Here the electron current is dominant over the ion current, and the greater the potential, the more electrons will escape to the probe and increase the measured current until the point where a further increase in potential difference merely increases the electrons' energies, with no effect on the current.

This point is known as the plasma potential, and from this data, appears to occur at around $3.5V$- In accordance with the result found by Robert L. Merlino in 2007 [9], which was $V_p \cong 4V$. The current value at which any increase in the probe voltage results in no further increase in the probe current is outlined by equation 2.6. One will note, however, that while the current is no longer increasing as in equation 2.5, the current does not plateau as had been predicted in figure 4. This could be due to the expansion of the negative sheath with increasing probe voltage, as more electrons obtain energies high enough to approach the probe. The sheath expansion [9] produces an increase in the total current, as the area over which the particles are collected is in fact the sheath and not the probe area.

Figure 4.2.2 shows a plot of the natural logarithm of the probe current versus the probe voltage in the range from $-4V$ to $+15V$. The figure shows the expected trend, with a linear increase in the natural logarithm of the probe current with probe voltage up to $3 \pm 0.5V$. Beyond this, the natural logarithm of current plateaus. This would suggest that the initial value for the plasma potential obtained from figure 4.2.1 is slightly overestimated. The gradual curve in said graph makes it difficult to identify this potential- but plotting a natural logarithm of the results clarifies this value.

From the relation in equation 2.5 and the gradient of the low voltage regime section of figure 4.2.2, the electron temperature can be determined. Upon solving for T_e in equation 2.5 one obtains the following expression:

$$\ln(I) = \frac{e}{k_B T_e} V$$

From the gradient of the plot, which was 1.38956 ± 0.04, the above expression was rearranged, and the electron temperature was found to be $\approx 8343.79 \pm 206.11K$ which is $\approx 0.72 \pm 0.02eV$. This is approximately half of that found by Robert L. Merlino, which was $\cong 1.5eV$. However, the result is very close to that found by I. Alexeff et al. in 1913, which was $0.9eV$ [13].

The electron density was also determined using the value for the electron saturation current. Rearranging equation 2.6, one obtains an expression which, upon determination of the electron saturation current, allows the electron density to be found:

$$n_e = \frac{I_{es}}{Ae\left({}^{kT_e}/_{2\pi m}\right)^{1/2}}$$

I_{es} was taken as the first value at which the trend in figure 4.2.1 plateaus. An accurate value is not able to be determined as the current continues to increase. However, the value estimated was taken at $5 \pm 0.5V$ and is approximately equal to $5 \pm 0.05mA$. Using these values and that for the electron temperature, the number density of electrons was found to be approximately $1.936 \times 10^{16} \pm 6.26 \times 10^{14} m^{-3}$. This is in close agreement with that found by Robert L. Merlino [9] who found the value to be $1.000 \times 10^{16} m^{-3}$.

6. Conclusion

For both parts of this investigation, the results are consistent with expectation, with the graph following the expected trend. For part 1, which involved the determination of the ionisation potential of argon, the plot of the voltage across the electrode versus the current through it to the power of 2/3 was as expected. Here, the Child-Langmuir law was well demonstrated, which states the effect of space charge between 2 parallel plate electrodes being that the applied voltage across the plates will therefore be proportional to $I^{2/3}$. Beyond this linear increase, the graph shows the now temperature-limited region governed by the Richardson-Dushman relation. The breakdown voltage, which is the potential at which this transition occurs, was determined to be $16.0 \pm 0.05V$ and thus the ionisation potential of Argon: $\approx 17.57 \pm 0.1V$. This is slightly higher than the expected result of $15.7V$ but is within acceptable range.

Part 2 of the investigation also produced results which obeyed the expected trend, with the I-V characteristic of the Langmuir probe showing the 2 regions of saturation and region of electron retardation. The exception being the lack of constant current value at the electron current saturation region. However, this ca be easily explained by sheath expansion effects. The electron temperature was determined as $\approx 8343.79K$ which is $\approx 0.72eV$. Again, this value is not quite as expected, based on the result found by Merlino in 2007 [9], which was $1.5eV$. From the second figure plotted for part 2, the plasma electron density was established as approximately $1.936 \times 10^{16} \pm 6.26 \times 10^{14} m^{-3}$. This is in close agreement with that found by Merlino, who found the value to be $1.000 \times 10^{16} m^{-3}$.

Overall, the experiment was successful in demonstrating the Child-Langmuir law for the diode used in part 1, and the I-V characteristic of the Langmuir probe. Amendments could be made in the timing of the reversal of polarity of the voltmeter and probe, as this may have offset the results slightly. The non-ideal behaviour of the probe and plasma resulted in difficulty upon establishing values such as the ion saturation current, however, logarithmic plots allowed for clarification of values such as this. The use of an argon gas-filled tube for both parts was beneficial in both its effectiveness of creating and demonstrating the behaviour of plasma parameters and the fact it is comparably easy to ionise. It is appropriate in a laboratory setting as it is the cheapest of all the noble gases. The results reflected the space-charge limited current for a particle moving at speeds which are non-relativistic. The behaviour of the current in the diode tube was indeed proportional to the three-halves power of the bias potential, while the behaviour of the current through the Langmuir probe was also proportional to the exponential of the voltage in the low voltage regime.

7. References

[1] The Langmuir-Child Law and the Work function of Tungsten. Devin Greene. Department of Physics and Engineering Physics, University of Saskatchewan, April 6, 2001

[2] A simple physical derivation of Child–Langmuir space-charge-limited emission using vacuum capacitance, R. J. Umstattd, C. G. Carr, C. L. Frenzen, J. W. Luginsland and Y. Y. Lau. American Journal of Physics, 2005

[3] Thermionic Emission. www.physics.csbsju.edu/370/thermionic.pdf

[4] Tutorial Particle sources 1 – Electron diode: Child-Langmuir law, T. Thuillier Juas, 2007.

[5] Space Charge Effects on Thermionic Emission: the Knee of the Transition from TL to FSCL Operation | Semantic Scholar https://www.semanticscholar.org/paper/Space-Charge-Effects-on-Thermionic-Emission%3A-the-of-Chan-Lu/16160eff860ced76c130e753e916b20f507d4d6f

[6] A new approach to the Child-Langmuir law, Gabriel Gonzalez and F.J. Gonzalez. 19th January 2012

[7] Plasma Physics - Two questions about Langmuir probe current-voltage characteristics - Physics Stack Exchange https://physics.stackexchange.com/questions/499082/two-questions-about-langmuir-probe-current-voltage-characteristics

[8] Digital smoothing of the Langmuir probe I-V characteristic. Magnus F, Gudmundsson JT. Science Institute, University of Iceland, Reykjavk, Iceland.

[9] Understanding Langmuir probe current-voltage characteristics, Robert L. Merlino, Department of Physics and Astronomy The University of Iowa, 14 July 2007

[10] Plasma, Gavin Cheung, January 27, 2012

[11] MSc Physics of Advanced Semiconductor Materials - lecture 4. Dr Paul May, Bristol University. 1998.

[12] An introduction to Langmuir probe diagnostics of plasmas, Luis Conde, Departamento de Física Aplicada, Universidad Politécnica de Madrid, Madrid, Spain, May 28, 2011

[13] Irving Langmuir, New elementary experiments in plasma physics, I. Alexeff, J. T. Pytlinski, N. L. Oleson, 1913